THE JOURNAL OF BIOLOGICAL CHEMISTRY
Vol. 271, No. 44, Issue of November 1, pp. 27879–27887, 1996
Printed in U.S.A.

Characterization of the AMP-activated Protein Kinase Kinase from Rat Liver and Identification of Threonine 172 as the Major Site at Which It Phosphorylates AMP-activated Protein Kinase*

(Received for publication, May 14, 1996, and in revised form, July 29, 1996)

Simon A. Hawley‡§, Matthew Davison¶, Angela Woods‖, Stephen P. Davies‡, Raj K. Beri¶, David Carling‖, and D. Grahame Hardie‡**

From the ‡Biochemistry Department, The University, Dundee DD1 4HN, Scotland, United Kingdom, ¶Zeneca Pharmaceuticals, Alderley Edge, Macclesfield SK10 4TG, United Kingdom, and the ‖Medical Research Council Molecular Medicine Group, Royal Postgraduate Medical School, Hammersmith Hospital, Du Cane Road, London W12 0NN, United Kingdom

We have developed a sensitive assay for the AMP-activated protein kinase kinase, the upstream component in the AMP-activated protein kinase cascade. Phosphorylation and activation of the downstream kinase by the upstream kinase absolutely requires AMP and is antagonized by high (millimolar) concentrations of ATP. We have purified the upstream kinase >1000-fold from rat liver; a variety of evidence indicates that the catalytic subunit may be a polypeptide of 58 kDa. The physical properties of the downstream and upstream kinases, *e.g.* catalytic subunit masses (63 *versus* 58 kDa) and native molecular masses (190 *versus* 195 kDa), are very similar. However, unlike the downstream kinase, the upstream kinase is not inactivated by protein phosphatases. The upstream kinase phosphorylates the downstream kinase at a single major site on the α subunit, *i.e.* threonine 172, which lies in the "activation segment" between the DFG and APE motifs. This site aligns with activating phosphorylation sites on many other protein kinases, including Thr^{177} on calmodulin-dependent protein kinase I. As well as suggesting a mechanism of activation of AMP-activated protein kinase, this finding is consistent with our recent report that the AMP-activated protein kinase kinase can slowly phosphorylate and activate calmodulin-dependent protein kinase I, at least *in vitro* (Hawley, S. A., Selbert, M. A., Goldstein, E. G., Edelman, A. M., Carling, D., and Hardie, D. G. (1995) *J. Biol. Chem.* 270, 27186–27191).

The AMP-activated protein kinase (AMPK)[1] is a protein kinase that phosphorylates multiple targets both *in vitro* and *in vivo* (1). These targets include several biosynthetic enzymes such as hydroxymethylglutaryl-CoA reductase (sterol/isoprenoid synthesis) (2, 3), acetyl-CoA carboxylase (fatty acid synthesis) (4–6), and glycogen synthase (glycogen synthesis) (7). The kinase is activated by elevation of the AMP:ATP ratio during cellular stress, and a current hypothesis for its physiological role is that it preserves ATP by switching off biosynthesis whenever cellular ATP levels are compromised by adverse cellular environments (8).

Purified AMPK consists of three subunits of 63, 38, and 35 kDa (9), now referred to as α, β, and γ, respectively (10). The catalytic (α) subunit (11) contains an N-terminal kinase domain and is closely related to the product of the *SNF1* gene from the yeast *Saccharomyces cerevisiae* (12, 13). A recent report (14) has identified a novel isoform, termed α_1, which is widely distributed, while the form originally cloned (Refs. 12, 15, and 16; now α_2) is highly expressed in heart, liver, and skeletal muscle. The functions of the β and γ subunits remain unknown, but both may also exist as multiple isoforms (14) and are related to the *SIP1*/*SIP2* and *SNF4* gene products, respectively, from *S. cerevisiae* (10). Snf4p has been shown to form a stable complex with Snf1p (17), while both Snf4p (18) and either Sip1p or Sip2p (19, 20) form complexes with Snf1p *in vivo* as assessed by the two-hybrid assay. Thus all three subunits of mammalian AMPK have counterparts in *S. cerevisiae*. Genetic evidence shows that functional *SNF1* (and *SNF4*) genes are required for the response to glucose starvation (17, 21), which in yeast could be regarded as an acute stress situation. In particular, Snf1p is required for derepression of genes that are normally repressed in the presence of glucose (21), while it is also required for inactivation of acetyl-CoA carboxylase, which occurs in response to starvation (22).

At present little is known about regulation of Snf1p, but the regulation of mammalian AMPK is better characterized. 5′-AMP not only allosterically activates the kinase but is also required for phosphorylation and activation by an upstream protein kinase termed AMP-activated protein kinase kinase (AMPKK) (23–25). Phosphorylation by AMPKK results in at least 50-fold activation, which can be further amplified by the 5-fold allosteric effect of AMP (25). We have also recently reported that micromolar concentrations of AMP dramatically inhibit dephosphorylation and inactivation of AMPK by protein phosphatase-2C (26).

* This study was supported by a Programme Grant from the Welcome Trust (to D. G. H.).

§ Supported by a Biotechnology and Biological Sciences Research Council Cooperative Award in Science and Engineering Research Studentship funded in part by the Medical Research Council Molecular Medicine Group. The costs of publication of this article were defrayed in part by the payment of page charges. This article must therefore be hereby marked "*advertisement*" in accordance with 18 U.S.C. Section 1734 solely to indicate this fact.

** To whom correspondence should be addressed: Biochemistry Dept., The University, Dundee DD1 4HN, Scotland, United Kingdom. Tel.: +44 1382 344253; Fax: +44 1382 201063; E-mail: d.g.hardie@dundee.ac.uk.

[1] The abbreviations used are: AMPK, AMP-activated protein kinase; AMPKK, AMP-activated protein kinase kinase; PP1, protein phosphatase-1; PP1γ, PP1, γ isoform; PP1γ_C, PP1γ catalytic subunit; PP2A, protein phosphatase-2A; PP2A$_C$, PP2A catalytic subunit; PP2A$_1$, ABC holoenzyme of PP2A from bovine heart; PP2C, protein phosphatase-2C; PP2Cα, PP2C, α isoform; SAMS synthetic peptide HMRSAMSGLHLVKRR; AMARA synthetic peptide AMARAASAAALARRR; PAGE, polyacrylamide gel electrophoresis; PEG, polyethylene glycol; FSBA, 5′-*p*-fluorosulfonylbenzoyladenosine; PTH, phenylthiohydantoin; CaMKI, calmodulin-dependent protein kinase I; HPLC, high pressure liquid chromatography.

Initially it was unclear whether the effect of AMP on phosphorylation of AMPK by AMPKK was due to binding of the nucleotide to the substrate (AMPK), to the enzyme (AMPKK), or to both. Although we reported that the former mechanism could explain the effect, at least in part (24), more recently we have presented evidence that AMP also activates AMPKK directly, *i.e.* that the latter is itself an AMP-activated protein kinase (27). An answer to this question was possible because we found that AMPKK would also phosphorylate and activate (at least *in vitro*) calmodulin-dependent protein kinase I, an enzyme that was not itself sensitive to AMP.

These findings show that the upstream protein kinase AMPKK plays an active role in the overall activation of the cascade by AMP rather than merely being a passive, constitutively active partner. This makes the further characterization of AMPKK an important goal. Here we report on the purification and some physical and regulatory properties of AMPKK, and we also identify the major site at which it phosphorylates and activates AMPK.

EXPERIMENTAL PROCEDURES

Materials—5′-AMP and ATP were from Boehringer (Lewes, UK). Phenylmethylsulfonyl fluoride, mannitol, benzamidine, palmitoyl-CoA, Brij-35, and *n*-octyl β-D-glucopyranoside were from Sigma (Poole, UK). Trypsin (modified sequencing grade) was from Promega (Southampton, UK). Optiscint Hisafe II, Optiphase, DEAE-Sepharose (Fast Flow), reactive blue-2-Sepharose, and prepacked Mono Q, Q-Sepharose, and Sephacryl S-200 columns were from Pharmacia (Milton Keynes, UK). Microcystin-LR (>98% pure) was from Calbiochem-Novabiochem (Nottingham, UK). Okadaic acid (Na^+ salt) was from Life Technologies (Paisley, UK). P-81 paper was from Whatman Labsales (Maidstone, UK). Centricon-30 concentrators were from Amicon, (Cirencester, UK). [γ-^{32}P]ATP and Hyperfilm-β_{max} were from Amersham International (Bucks, UK). [^{14}C]FSBA was from NEN, (Stevenage, UK). All other reagents were Analar grade from BDH (Poole, UK).

Proteins and Peptides—5′-Nucleotidase (from *Crotalus adamateus* venom) bound to agarose, soybean trypsin inhibitor (type II-S), SDS-PAGE, and gel filtration markers were from Sigma. Bovine brain calmodulin was from Boehringer. Prestained "rainbow" molecular weight markers were from Amersham. Rabbit protein phosphatase-1γ_C (28) and human protein phosphatase-2Cα (26) were bacterially expressed proteins and were gifts from Dr. P. T. W. Cohen. Protein phosphatases LAR (29), CL-100 (30), and 2A_1 (ABC holoenzyme from bovine heart, purified as for rabbit muscle (31)) were gifts from David Barford (Oxford University), Steve Keyse (Dundee University), and Nick Morrice (MRC Protein Phosphorylation Unit, Dundee). Protein phosphatase-2A_C (PP2A_C, catalytic subunit) was purified from bovine heart as described previously for rabbit muscle (31). The "SAMS" and "AMARA" peptides (32) were synthesized and purified as described previously. AMPK-α antiserum was raised against the peptide PGLKPHPERMPPLI (residues 361–374 of AMPK-α2 (12)) and affinity-purified using the peptide antigen. AMPK-β antiserum was raised against bacterially expressed β subunit (33).

Buffers—The protease inhibitors benzamidine (1 mM), soybean trypsin inhibitor (1 μg/ml), and phenylmethylsulfonyl fluoride (1 mM) were added to buffers A, B, C, and D immediately prior to use (buffer A: 0.05 *I* Tris/HCl, pH 8.4, at 4 °C, 0.25 M mannitol, 50 mM NaF, 5 mM sodium pyrophosphate, 1 mM EDTA, 1 mM EGTA, 1 mM dithiothreitol; buffer B: 0.05 *I* Tris/HCl, pH 7.4 at 4 °C, 0.25 M mannitol, 50 mM NaF, 5 mM sodium pyrophosphate, 1 mM EDTA, 1 mM EGTA, 0.02% (w/v) Brij-35, 10% (v/v) glycerol, 1 mM dithiothreitol; buffer C: as buffer B but without NaF and sodium pyrophosphate; buffer D: buffer C plus 0.1 M NaCl, 50 mM $MgCl_2$; buffer E: 50 mM Na-Hepes, pH 7.0, 0.02% (w/v) Brij-35, 1 mM dithiothreitol.

Enzyme Assays—PP2A was assayed using phosphorylase *a* (31). One unit of PP2A dephosphorylates 1 μmol of substrate/min at 30 °C. AMPK was assayed as described (34) except that, unless stated otherwise, the AMARA peptide (200 μM) replaced SAMS. One unit of AMPK phosphorylates 1 μmol of peptide/min at 30 °C. AMPKK was assayed by its ability to reactivate dephosphorylated AMPK; a single preparation of AMPK was used throughout these studies. The preparation was stored frozen at −70 °C in small aliquots at 10 units/ml in buffer C. Before use it was diluted to 2 units/ml in buffer C containing 50% glycerol; in this form it could be stored at −20 °C for up to a month. AMPK (0.013 units/ml in buffer E) was inactivated by incubation with PP2A_C (6 milliunits/ml final concentration) at 30 °C for 10 min. PP2A was inhibited by the addition of okadaic acid to 100 nM final. Three volumes of dephosphorylated AMPK were added to 1 volume of ATP, $MgCl_2$, and AMP in buffer E, and 3 volumes of this mixture was added to 1 volume of AMPKK in buffer E. Final concentrations were 1 mM ATP, 5 mM $MgCl_2$, and 100 μM AMP. The reaction was incubated at 30 °C, and 5-μl aliquots were removed at 0 and 25 min for the AMPK assay as described above. One unit of AMPKK was that amount which increased the activity of dephosphorylated AMPK by 1 unit/ml (calculated at the dilution of the stock AMPK) per min at 30 °C.

Protein Analysis and Electrophoresis—Protein concentration was determined by the method of Bradford (35). SDS-PAGE was on 10% gels using the method of Laemmli (36) in a Bio-Rad Mini-Protean II gel apparatus unless stated otherwise.

Purification of AMPK—AMPK was purified using modifications of the previous method (11). All procedures were at 4 °C unless stated otherwise. Livers from male Wistar rats were left at room temperature for 1–2 min to become hypoxic (this elevates AMP and activates AMPK (5)), chopped coarsely, and washed in buffer A. A 2.5–6% polyethylene glycol 6000 (PEG) fraction was prepared as described (11), resuspended in buffer B using a ground glass homogenizer, and applied to a DEAE-Sepharose (Fast Flow) column (6 × 15 cm). The column was washed until $A_{280} < 0.05$, and protein was eluted with buffer B plus 0.2 M NaCl. Active fractions were loaded directly onto blue-Sepharose (5 × 7 cm) and washed extensively, and protein was eluted with buffer B plus 0.8 M NaCl. Active fractions were precipitated with ammonium sulfate, resuspended, and dialyzed as for the previous procedure (11) and then clarified by centrifugation (20,000 × *g*, 10 min). The preparation was applied to a Q-Sepharose HiLoad 16/10 column at 3 ml/min, the column was washed until A_{280} was <0.05, and protein was eluted with a linear gradient from 0 to 450 mM NaCl in buffer B. Active fractions were pooled, concentrated to <0.5 ml in Centricon-30 concentrators, and applied to a high performance Sephacryl S-200 HiLoad column in buffer C at 0.5 ml/min. Active fractions were pooled, concentrated to 10 units/ml in Centricon-30 concentrators, frozen in small aliquots in liquid N_2, and stored at −70 °C.

Purification of AMPKK—All procedures were at 4 °C unless stated otherwise. The 6% PEG supernatant from the AMPK preparation above was made to 10% (w/v) PEG and centrifuged (30,000 × *g*, 20 min). The pellet was resuspended in buffer B and applied to a DEAE-Sepharose (Fast Flow) column (6 × 15 cm). The column was washed until A_{280} was <0.05, and protein was eluted with buffer B plus 0.2 M NaCl. Active fractions were loaded directly onto Blue-Sepharose (5 × 7 cm), and the flow-through was applied to a high performance Q-Sepharose HiLoad 16/10 column in buffer B plus 200 mM NaCl at 3 ml/min. The column was washed until A_{280} was <0.05 and then AMPKK was eluted with a 96-ml linear gradient from 200 to 500 mM NaCl in buffer B. Active fractions were pooled, concentrated to <0.5 ml in Centricon-30 concentrators, diluted 3-fold in buffer C, and applied to a Mono Q (HR 5/5) column at 1 ml/min. The column was washed until A_{280} was <0.05, and then AMPKK was eluted with gradients from 0 to 50 mM $MgCl_2$ (1 min) and 50–100 mM $MgCl_2$ (24 min) in buffer C. Active fractions were pooled, concentrated to <0.5 ml in Centricon-30 concentrators, and then diluted 3-fold in buffer D. An ATP-γ-Sepharose (9) column (1.5 ml) was equilibrated in buffer D. AMPKK was applied, stirred into the matrix, and allowed to stand for 20 min. The column was washed at ~1 ml/min with 40 ml of buffer D and then 25 ml of buffer D plus 5 mM ATP. Active fractions were pooled, concentrated in Centricon-30 concentrators, frozen in small aliquots in liquid N_2, and stored at −70 °C. Aliquots of the Q-Sepharose fraction were stored in the same way and used in some experiments (Figs. 1 and 4–10).

Determination of Physical Parameters of AMPKK—AMPKK (250 μl, 200 units/ml, Q-Sepharose preparation) was subject to gel filtration on a Sephacryl S-200 column (60 × 1.6 cm) in buffer B, both in the presence and absence of 0.2 M NaCl. The column was calibrated prior to use, using markers of known Stokes radii (Sigma gel filtration markers). For gradient centrifugation, AMPKK (amount and purity as for gel filtration) was layered with or without marker proteins (8.9 S sweet potato β-amylase and 4.4 S bovine serum albumin) onto a glycerol gradient (10–20% (v/v), 14 ml) in buffer B. A third tube contained marker proteins alone. The tubes were centrifuged in a Beckman SW 28 rotor (100,000 × *g*, 42 h, 4 °C). Fractions (0.5 ml) were collected from the bottom of the tube using a Nyegaard gradient unloader and analyzed for protein (A_{280}) and AMPKK activity.

Labeling of AMPKK Using [γ-^{32}P]ATP or [^{14}C]FSBA—AMPKK (125 μg/ml, ATP-γ-Sepharose preparation in buffer E) was incubated at 30 °C for 40 min with either (a) 200 μM [γ-^{32}P]ATP (1.5 × 10^6 cpm/nmol) or (b) 200 μM of [^{14}C]FSBA (80,000 dpm/nmol). Reactions were stopped

by the addition of SDS-PAGE sample buffer. Autoradiography (ATP labeling) was performed on dried gels at −70 °C using Hyperfilm-β max with Kodak X-Omatic intensifying screens. Phosphor imaging (FSBA labeling) was performed using a Molecular Dynamics PhosphorImager.

Protein Phosphatase Treatment of AMPKK—AMPKK (770 units/ml) was incubated with protein phosphatases $PP2A_C$ (50 milliunits/ml), $PP2A_1$ (50 milliunits/ml), PP1γ (50 milliunits/ml), PP2C (1.5 milliunits/ml), CL-100 (6 μg/ml), or LAR (6 milliunits/ml) for 20 min at 30 °C in buffer C.

Phosphorylation and Immunoprecipitation of AMPK for Sequencing Studies—AMPK was purified to the gel filtration step as described above, except that NaF and sodium pyrophosphate were omitted from the gel filtration buffer. AMPK (14,000 units) was dephosphorylated using $PP2A_C$ (500 milliunits) for 15 min at 30 °C in 8 ml of buffer C. The reaction was stopped by adding okadaic acid to 100 nM, and then incubation was continued for 8 min in the presence of AMP (100 μM), $MgCl_2$ (5 mM), and [γ-^{32}P]ATP (200 μM; 400 cpm/pmol) in the presence or absence of AMPKK (210 units). Reactivation was terminated by the addition of EDTA to 20 mM, and then AMPK was immunoprecipitated by five sequential additions of anti-AMPK-β subunit antibody. In each case, 200 μl of a 50% (v/v) slurry of protein A-Sepharose in buffer B containing 1% (w/v) Triton X-100 was added, and the resulting mixture was incubated for 2 h at 4 °C with constant shaking. The immunocomplex was collected by centrifugation and washed extensively with buffer B containing 1% (w/v) Triton X-100. The immunoprecipitates were combined, boiled with SDS-PAGE sample buffer, resolved by SDS-PAGE on 10% gels, and transferred electrophoretically to polyvinylidene difluoride membranes (37).

Tryptic Digestion of AMPK and Purification of ^{32}P-Peptides for Sequencing Studies—Peptides were digested on polyvinylidene difluoride membranes using trypsin (37). The membranes were stained with sulforhodamine (Eastman Kodak Co.) (38). Regions of the membrane containing the α and β subunits were excised, cut into ~4 × 4-mm pieces, and incubated with sufficient trypsin solution (100 μg/ml in 200 mM NH_4HCO_3 containing 1% (w/v) *n*-octyl β-D-glucopyranoside) to fully wet the membranes. After 24 h at room temperature, 0.1 volume of 100 mM dithiothreitol in buffer A was added, and incubation continued for a further 24 h. The membrane pieces were extracted once with 0.6–1.0 ml of buffer A, followed by transfer of the supernatant to clean polypropylene tubes. This first extract contained about 70% of the total counts; subsequent extraction of the membrane pieces with the same volume of buffer A and then the same volume of 50% formic acid:methanol resulted in extraction of a further 15 and 8% respectively. These extracts were dried on a rotary evaporator and resuspended in 200–300 μl of 0.1% (v/v) trifluoroacetic acid. In order to keep the octyl glucoside concentration below 2% (w/v), to 50-μl aliquots of these samples 10 μl of 100 mM dithiothreitol was added followed by 50 μl of 0.1% (v/v) trifluoroacetic acid and then 10 μl of 10% (v/v) trifluoroacetic acid. Aliquots were then subjected to reversed phase HPLC using a 2.1 × 100-mm Aquapore OD300 C18 column (Applied Biosystems) at a flow rate of 250 μl/min. Fractions were collected at 1-min intervals. The column was washed with 0.1% (v/v) trifluoroacetic acid in acetonitrile:water (3:97) for 5 min, followed by a gradient (5–90 min) from 3 to 60% of 0.1% (v/v) trifluoroacetic acid in acetonitrile:water (9:1). Some of the radioactive peaks from these initial runs were pooled, dried by rotary evaporation, and resuspended in 50 μl of buffer F (10 mM ammonium acetate pH 6.5) followed by 10 μl of 10 mM dithiothreitol and 60 μl of 200 mM ammonium acetate, pH 6.5. Peptides were separated by reversed phase HPLC as before except using buffer F in place of 0.1% trifluoroacetic acid. Recovery of radioactivity from HPLC in either buffer was 50–70%.

Amino Acid Sequencing—Fractions containing radiolabeled peptides were pooled and dried down onto a Sequelon arylamine membrane disc (Millipore Corp.). The peptides were coupled to the disc according to manufacturer's instructions, and the discs were washed with 1 ml of 50% (v/v) methanol followed by 1 ml of 0.1% (v/v) trifluoroacetic acid in 50% (v/v) acetonitrile. Coupling efficiencies, as determined by counting of radioactivity, were ~90%. The membrane discs were subjected to N-terminal sequencing using a modified ABI 475 gas phase sequencer, which either injected 100 out of 120 μl of the PTH-derivative into the HPLC analyzer or delivered the whole fraction into a fraction collector. Solvent S3 was 70% (v/v) acetonitrile. The radioactivity in the PTH-derivative fraction was determined by scintillation counting using a Wallac 1218 counter.

RESULTS

Establishment of an Assay for AMP-activated Protein Kinase Kinase—Purification and characterization of AMPKK required the development of a sensitive and quantitative assay. We utilized its ability (24) to catalyze the time- and MgATP-dependent reactivation of purified AMPK, which had been inactivated by pretreatment with the purified catalytic subunit of protein phosphatase-2A ($PP2A_C$). We found it necessary to perform the protein phosphatase treatment immediately prior to the AMPKK assay, since the dephosphorylated form of AMPK appears to be unstable on storage. After the protein phosphatase treatment, okadaic acid was added to prevent the protein phosphatase interfering with the two subsequent kinase reactions. Fig. 1 shows that this reactivation is suitable for a quantitative assay using a crude postmitochondrial supernatant fraction from rat liver, a PEG precipitate prepared from it, or a much more highly purified fraction (Q-Sepharose). With crude fractions, the assay became nonlinear with protein concentration when the degree of reactivation was >30%. Remarkably, after purification through four steps (Q-Sepharose fraction) the assay was essentially linear right up to 100% reactivation.

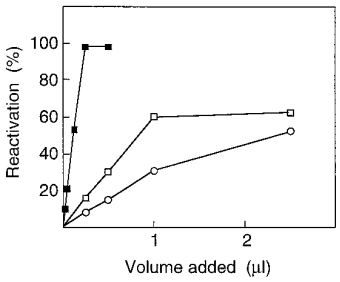

FIG. 1. **Validation of AMPKK assay.** Dependence of reactivation of AMPK on the volume of AMPKK fraction added for the postmitochondrial (10,000 × *g*) supernatant (*open circles*), the 6–10% PEG precipitate (*open squares*), and the Q-Sepharose fraction (*filled squares*) is shown. AMPK activity is expressed as a percentage of the activity observed before inactivation by $PP2A_C$.

In the initial studies, we assayed AMPK after reactivation using as substrate the synthetic SAMS peptide (HMRSAMSGLHLVKRR), which is based on the primary phosphorylation site on rat acetyl-CoA carboxylase (34). However, as we purified AMPKK further this substrate began to give high blanks, *i.e.* there was significant phosphorylation of the peptide even if dephosphorylated AMPK was not added. This was eventually traced to the presence of protein kinase(s) that co-purified with AMPKK. The problem of the high blanks could be overcome by replacing SAMS with the peptide AMARAASAAALARRR, which we developed as a basis for specificity studies on AMPK and its homologues (32). Not only is this a better substrate for AMPK (V/K_m 5-fold higher), but it was not a substrate at all for the SAMS kinase(s) that contaminated the AMPKK preparation. All subsequent studies were conducted using this peptide to assay the reactivated AMPK.

Purification of AMPKK—In previous studies (24) AMPKK had been detected as a byproduct of the AMPK preparation. It had been partially purified from the 2.5–6% PEG precipitate used in the AMPK purification, being resolved from AMPK at the third step (blue-Sepharose). With our new more quantitative assay we reexamined the recovery of AMPKK in the early stages of the procedure and found that only a small proportion of the total activity was recovered in the 2.5–6% PEG precipitate. The majority of AMPKK was in the 6–10% PEG precipitate, which was therefore used as the starting point for further purification. A six-step procedure, utilizing affinity chromatography on ATP-γ-Sepharose (9, 39) as the final step, resulted in >1000-fold purification of AMPKK from a postmitochondrial supernatant fraction of rat liver (Fig. 2, Table I). Despite prolonged efforts, we were unable to achieve further purification

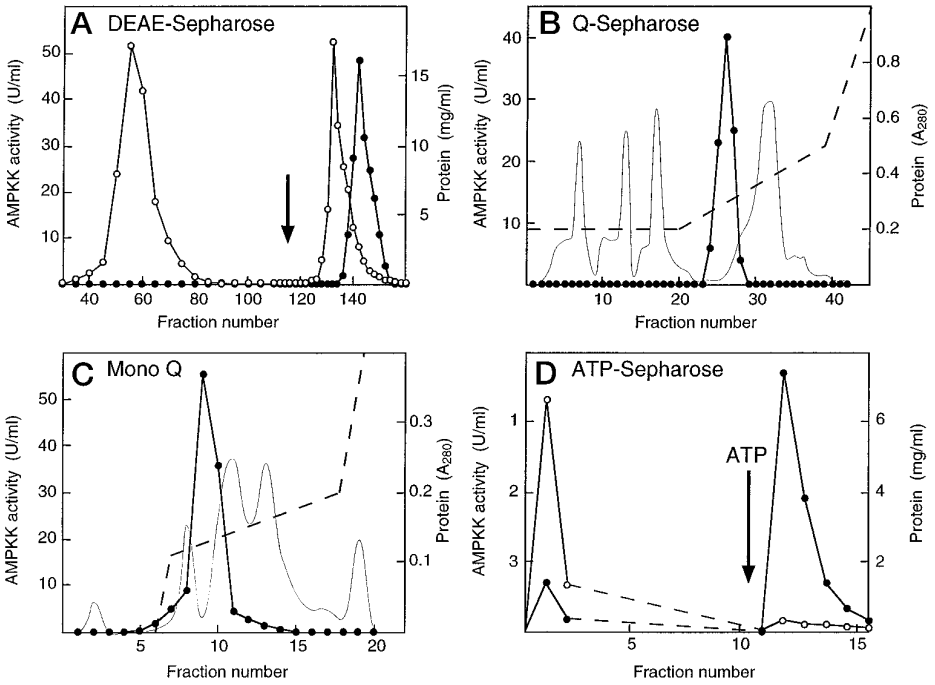

FIG. 2. **Purification of AMPKK (*filled circles*) on DEAE-Sepharose (*A*), Q-Sepharose (*B*), Mono Q (*C*), and ATP-γ-Sepharose (*D*).** Also shown is the protein concentration determined by Coomassie Blue binding (*open circles* in *A* and *D*) or A_{280} (*continuous line* in *B* and *C*).

TABLE I
Purification of AMPKK from rat liver

Data are results from a preparation using livers of 20 male rats (~300 g, wet weight). AMPKK was determined by reactivation of AMPK, using the AMARA peptide to assay the latter. Protein concentration was determined by Coomassie Blue binding (35).

Fraction	Protein	Total AMPKK	Specific activity	Purification	Yield
	mg	*units*	*units/mg*	*-fold*	*%*
Postmitochondrial supernatant	50,561	4928	0.098	1	100
2.5% PEG supernatant	29,929	4779	0.6	1.6	97
6–10% PEG precipitate	3904	4206	1.08	11	85
DEAE-Sepharose	1004	3400	3.4	35	69
Blue-Sepharose	832	2850	3.4	35	58
Q-Sepharose	32.4	565	17.4	178	11.5
Mono Q ($MgCl_2$ gradient)	2.2	67	31	313	1.4
ATP-γ-Sepharose	0.28	28	101	1032	0.6

by conventional means. Further studies were therefore conducted with this preparation.

Molecular Mass of AMP-activated Protein Kinase Kinase and Its Catalytic Subunit—SDS-PAGE revealed that the preparation still contained several polypeptides, but with a species of apparent molecular mass 58 kDa being a major component (Fig. 3, *lane 1*). When incubated with [γ-^{32}P]ATP, this polypeptide was essentially the only labeled species (Fig. 3, *lane 2*). We also conducted experiments aimed at identification of the catalytic subunit using the reactive ATP analogue FSBA. This reagent inactivates the catalytic subunit of cyclic AMP-dependent protein kinase by reacting with the lysine residue (40) that is conserved in the ATP binding site of all other protein kinases (41). As expected, FSBA caused a time-dependent, exponential decay of AMPKK activity, with half-times of 18 min at 250 μM, and 43 min at 100 μM FSBA (data not shown). Using [^{14}C]FSBA, the 58-kDa polypeptide was the only significant radioactive species detectable after an SDS-PAGE gel was analyzed by PhosphorImager analysis (Fig. 3, *lane 3*). The radioactivity migrating at the dye front was also evident in a control incubated without AMPKK (not shown) and is due to unreacted [^{14}C]FSBA or its breakdown products.

We also estimated the native molecular mass (42) of AMPKK by combining the Stokes radius determined by gel filtration (5.5–5.7 nm; Fig. 4) and the sedimentation coefficient determined by glycerol gradient centrifugation (8.4–8.6 S; Fig. 5), which yielded a value of 196 ± 5 kDa. The frictional ratio (f/f_0) was 1.44–1.47, indicating that AMPKK has a highly asymmetric structure. Prolate or oblate ellipsoids of this frictional ratio would have axial ratios of ~8 and ~10, respectively. The migration of AMPKK on gel filtration was not affected by the presence or absence of 0.2 M NaCl in the buffer (not shown).

Dependence of AMPKK on AMP and ATP and Lack of Effect of Protein Phosphatases—We have previously reported that reactivation of AMPK by AMPKK is absolutely dependent on the presence of 5′-AMP (24). In the present study we examined whether the effect of AMP on the AMPKK reaction could be antagonized by high concentrations of ATP. Fig. 6 (*open circles*) shows the effect of varying the ATP concentration, at a constant AMP concentration of 100 μM, during the AMPKK assay. Rather than the simple hyperbolic curve one might expect for a protein kinase reaction, a more complex curve was obtained, with ATP completely inhibiting the reaction at high concentration. The data could be fitted to a model in which ATP bound with positive cooperativity at the catalytic site(s) (half-maximal activation at 16 ± 6 μM; Hill coefficient (h) = 1.6 ± 0.5) but also bound at higher concentration at inhibitory allosteric site(s) (half-maximal inhibition at 360 ± 80 μM; h = 1.9 ± 0.4). These results show that, as for the allosteric effect of AMP on AMPK itself (11, 25), the activation of AMPK by AMPKK in the presence of AMP is antagonized by high concentrations of ATP. When the experiment was performed at a higher AMP concentration (500 μM; Fig. 6, *filled circles*), the whole curve was shifted to the right; half-maximal activation was now at 54 ± 4

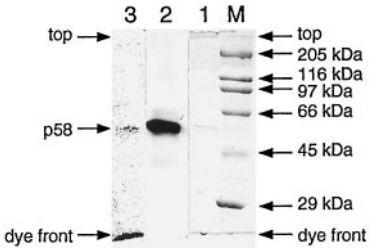

FIG. 3. **Analysis of purified AMPKK by SDS-polyacrylamide gel electrophoresis.** The γ-ATP-Sepharose-purified preparation was allowed to autophosphorylate using [γ-^{32}P]ATP and was separated by SDS-PAGE, and the gel was analyzed by Coomassie Blue staining (*lane 1*) and autoradiography (*lane 2*). *Lane 3* shows a similar sample analyzed on the PhosphorImager after labeling with [^{14}C]FSBA: the radioactivity migrating at the dye front was also observed in a control incubated without AMPKK (not shown). Marker proteins were separated in *lane M* (Sigma high molecular weight markers), with the molecular masses in kDa shown on the *right*.

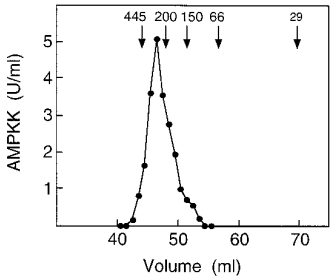

FIG. 4. **Recovery of AMPKK activity (*filled squares*) after gel filtration on a column (60 × 1.6 cm) of Sephacryl S-200.** The AMPKK loaded (50 units) was purified as far as the Q-Sepharose step. Migration of marker proteins (horse spleen apoferritin, 445 kDa; sweet potato β-amylase, 200 kDa; yeast alcohol dehydrogenase, 150 kDa; bovine serum albumin, 66 kDa; carbonic anhydrase, 29 kDa) is indicated by *arrows*.

μM ATP (h = 1.6 ± 0.2), and half-maximal inhibition was at 910 ± 50 μM ATP (h = 2.0 ± 0.2). At high concentrations, AMP can therefore antagonize binding of ATP at both the catalytic and allosteric sites.

Since results in this study suggested that AMPKK and AMPK have several remarkable similarities, we considered the possibility that, like AMPK, AMPKK might be regulated by reversible phosphorylation. To examine this possibility, we incubated AMPKK with purified preparations of protein serine/threonine phosphatases ($PP2A_C$, $PP2A_1$, PP2Cα, $PP1\gamma_C$), a protein-tyrosine phosphatase (LAR), and a dual specificity protein phosphatase (CL-100). Although all were active against known substrates (see "Experimental Procedures" for further details), none had any effect on the activity of AMPKK (not shown).

Identification of the Activating Phosphorylation Site Phosphorylated by AMPKK on AMPK—In order to determine the site of activating phosphorylation, AMPK was dephosphorylated with $PP2A_C$ and incubated with AMPKK in the presence of [γ-^{32}P]ATP. The AMPKK preparation was not homogeneous and gave a fairly high background phosphorylation when incubated on its own (see Ref. 27). We therefore reisolated AMPK after phosphorylation, by immunoprecipitation using anti-β subunit antibody. When AMPK was dephosphorylated and incubated with AMP and [γ-^{32}P]ATP alone, autophosphorylation occurred principally on the α subunit, with traces on the β and γ subunits (Fig. 7); there was no activation under these conditions (not shown). When AMPKK was added to the incubation, phosphorylation of the α subunit increased (although this may not be obvious in Fig. 7 due to the high autophosphorylation) and was accompanied by >95% reactivation of AMPK as expected. There was also increased labeling of the β subunit.

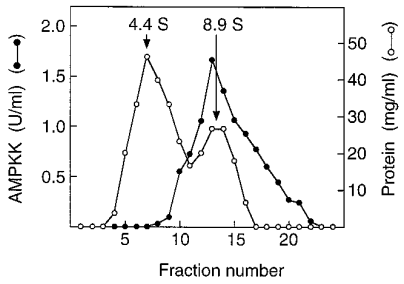

FIG. 5. **Glycerol gradient centrifugation of AMPKK.** A sample of AMPKK identical to that used in Fig. 4 (50 units) was sedimented through a glycerol gradient (*left* to *right*) as described under "Experimental Procedures." The gradient was fractionated and analyzed for AMPKK activity (*filled circles*) and protein concentration (*open circles*). AMPKK was run both in the presence and absence of marker proteins (sweet potato β-amylase, 8.9 S; bovine serum albumin, 4.4 S). The sedimentation of AMPKK was identical in the presence and absence of these markers, and *vice versa*. The protein profile shown was obtained from a third gradient run at the same time in the absence of AMPKK.

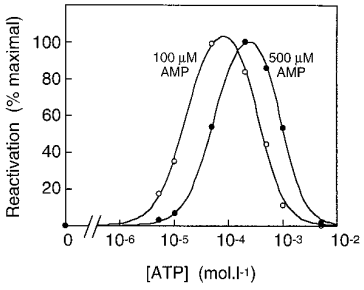

FIG. 6. **Effect of ATP concentration on the reactivation of AMPK by AMPKK, using either 100 μM (*open circles*) or 500 μM (*filled circles*) AMP.** During the AMPKK assays, $MgCl_2$ was maintained at a constant excess of 25 mM above [ATP]. During the subsequent AMPK assay, $MgCl_2$ and ATP were normalized at 30 mM and 1.2 mM. *Circles* show the experimental data; the curves represent theoretical fits to the equation $v = Max\cdot[ATP]^{n1}/(A_{0.5}{}^{n1} + [ATP]^{n1}) - Max\cdot[ATP]^{n2}/(I_{0.5}{}^{n2} + [ATP]^{n2})$. *Max* is the theoretical activity when the activating site is fully occupied and the inhibitory site is empty, $A_{0.5}$ is the concentration giving a half-maximal effect at the activating site, $I_{0.5}$ is the concentration giving a half-maximal effect at the inhibitory site, and *n1* and *n2* are Hill coefficients. Estimates, with standard errors, of these parameters are given under "Results." Curve fitting was carried out using Kaleidagraph (Abelbeck Software).

When AMPK was incubated with AMPKK in the presence of AMP and [γ-^{32}P]ATP, an additional labeled polypeptide with an apparent molecular mass of ~58 kDa became evident in the anti-β subunit immunoprecipitate (Fig. 7). This corresponded to p58, the major autophosphorylated polypeptide in the AMPKK preparation (Fig. 3). The labeled p58 was not precipitated by the anti-β subunit antibody in the absence of AMPK (not shown). Unfortunately, p58 was not clearly resolved from the immunoglobulin heavy chain on the Coomassie-stained gel, so it was not possible to estimate its abundance relative to the AMPK subunits.

The α subunit labeled in the presence or absence of AMPKK was purified by SDS-PAGE followed by electrophoretic transfer to polyvinylidene difluoride membrane. The polypeptide was digested on the membrane with trypsin as described under "Experimental Procedures." Fig. 8 shows the resolution of phosphopeptides obtained by reversed phase HPLC in 0.1% trifluoroacetic acid for the AMPKK-treated sample and for the autophosphorylation control. In addition to a small peak of radioactivity in the column breakthrough, autophosphorylation of AMPK gave rise to four radiolabeled peptide peaks (labeled *1–4* in Fig. 8, with *peak 1* being a shoulder on the leading edge of *peak 2*). Peaks 1–4 were also seen in very similar amounts when AMPK was incubated with AMPKK, but

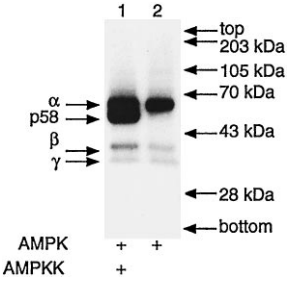

FIG. 7. **Autoradiogram showing co-precipitation of AMPKK and AMPK.** AMPK was incubated with [γ-^{32}P]ATP in the presence (*lane 1*) or absence (*lane 2*) of AMPKK and immunoprecipitated with anti-β subunit antibody as described under "Experimental Procedures." The immunoprecipitate was analyzed by SDS-PAGE (10% gel), and the gel was dried and exposed to x-ray film. Migration of marker proteins (prestained markers, Life Technologies) is indicated on the *right*.

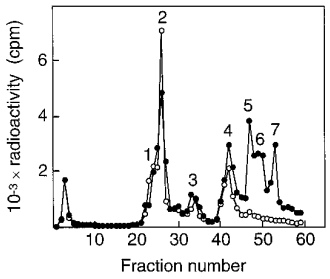

FIG. 8. **Reversed phase HPLC of ^{32}P-peptides derived from the AMPK α subunit phosphorylated using [γ-^{32}P]ATP in the presence (*filled circles*) and absence (*open circles*) of AMPKK.** Tryptic digests were prepared as described under "Experimental Procedures" and analyzed on a C18 column in 0.1% (v/v) trifluoroacetic acid using a gradient from water to acetonitrile. The flow rate was 250 μl/min, and 250-μl fractions were collected. Radioactivity was determined by Cerenkov counting of fractions.

three new peaks (peaks 5, 6, and 7) were also seen eluting later in the gradient. Similar results were obtained in three experiments with different preparations of both AMPK and AMPKK, except that the distribution of radioactivity between trifluoroacetic acid peaks 5, 6, and 7 was somewhat variable, with peaks 6 and 7 being less prominent in other runs.

Trifluoroacetic acid peaks 5, 6, and 7 were each further purified by reversed phase HPLC in ammonium acetate, pH 6.5. In each case up to three closely eluting radioactive peaks were obtained, termed AA1–AA3 (not shown). Trifluoroacetic acid peak 5 yielded predominantly AA1, trifluoroacetic acid peak 6 a mixture of AA1 and AA2, and trifluoroacetic acid peak 7 a mixture of AA2 and AA3. The AA1 peaks from trifluoroacetic acid peaks 5 and 6 were combined, coupled through the C terminus to a Sequelon membrane, subjected to solid phase sequencing, and found to yield the single sequence IA*X*F-GLS*X*MMS*X*G*X*FLR (Fig. 9*A*), corresponding unequivocally to the N-terminal sequence of the predicted tryptic peptides from Ile^{155} to Arg^{171} in AMPK-α_2 (12) or AMPK-α_1 (14). Three of the unassigned residues could be accounted for by predicted acidic amino acids (Asp^{157}, Asp^{166}, Glu^{168}), which would be expected to yield blank cycles due to the coupling of the peptide to the filter disc through carboxyl groups. Counting of the PTH-derivative fractions from this run (Fig. 9*A*) showed that there was a small peak of radioactivity at cycle 7, corresponding to Ser^{161}, followed by a larger peak at cycle 18, corresponding to Thr^{172}. Trypsin apparently had not cleaved the peptide at Arg^{171}, probably due to the proximity of the phosphate group on Thr^{172}.

Although the radioactivity in cycle 7 in Fig. 9*A* might appear to be fairly substantial, after correction for the amounts of PTH-derivative being recovered at the respective stages of the

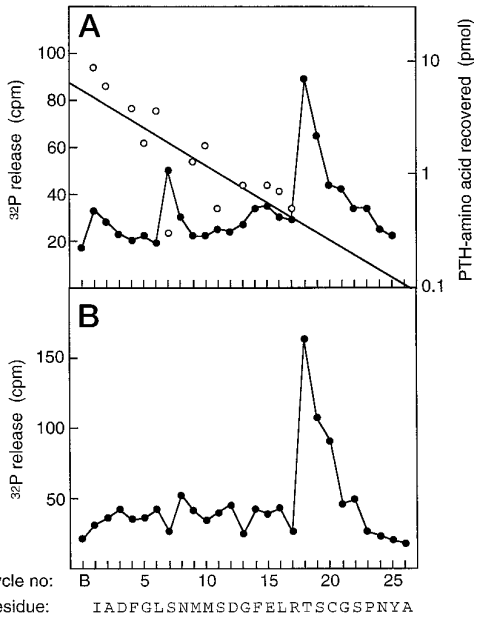

FIG. 9. **Recovery of radioactivity (*filled circles*) and semilogarithmic plot of recovery of PTH-derivatives (*open circles*) *versus* cycle number during solid phase sequencing of peptide 5.** *Panel A* shows results obtained from the preparation depicted in Fig. 8; the AA1 peaks derived from trifluoroacetic acid peaks 5 and 6 were combined for analysis. *Panel B* shows results from another preparation of trifluoroacetic acid peak 5 where the second (pH 6.5) HPLC run was omitted and only the recovery of radioactivity was determined. The *abscissa* is marked with the cycle number (*B* refers to counting of a reagent blank) and the residue, which is the single letter code of the predicted N-terminal sequence of the tryptic peptide from Ile^{154} to Ala^{190} of AMPK-α_1 or AMPK-α_2: residues of this sequence identified are shown by *open circles* in *panel A*). Aspartic and glutamic acid residues were not detected because the peptide was coupled to the filter via carboxyl residues, so cycles 3, 12, and 15 yielded blanks as expected. The residue at cycle 8 (Asn expected) was not identified due to a problem with injection of the PTH-derivative onto the HPLC. The *straight line* shows fitting of the PTH-amino acid recovery to an exponential decay with a repetitive yield of 86%.

sequencer run, it only accounted for 6% of the radioactivity loaded, whereas cycle 18 accounted for ~80%. When the amount of radioactivity in each of these cycles was converted into picomoles and compared with the pmol of PTH-derivative recovered, the stoichiometry of phosphorylation was ~3% at Ser^{161} and >45% at Thr^{172}. The low stoichiometry of phosphorylation at Ser^{161} is also confirmed by the recovery of substantial amounts of PTH-serine in cycle 7 (where the amino acid is serine, the recovery of PTH-serine is usually <50% of that obtained for most other amino acids, whereas if it is phosphoserine, no PTH-serine is recovered). In addition, in another preparation of AA1 no radioactivity was recovered at cycle 7 (Fig. 9*B*).

Some radioactivity was also recovered in cycle 19 and, with one preparation, in cycle 20 (Fig. 9), corresponding to Ser^{173} and Cys^{174}, respectively. While it is not possible to rule out a slight phosphorylation of Ser^{173}, we think these results are most likely explained by carry over of Thr^{172} into cycles 19 and 20, due to the repetitive yield being less than 100%. In the run shown in Fig. 9*A*, the carry over of the PTH amino acid from cycle 15 into cycle 16 was >30%.

Sequencing of peak AA2 (pooled from runs derived from trifluoroacetic acid peaks 6 and 7) yielded the same major sequence as for peak 5. Once again the radioactivity was released in cycle 18 during solid phase sequencing (data not shown). There was insufficient material in peak AA3 to allow sequence determination.

Fig. 10 shows separation of phosphorylated tryptic peptides

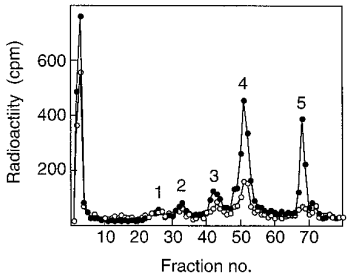

FIG. 10. **Reversed phase HPLC of ^{32}P-peptides derived from the AMPK β subunit phosphorylated using [γ-^{32}P]ATP in the presence (*filled circles*) and absence (*open circles*) of AMPKK.** Tryptic digests were prepared as described under "Experimental Procedures" and analyzed on a C18 column in 0.1% (v/v) trifluoroacetic acid using a gradient from water to acetonitrile. The flow rate was 250 μl/min, and 250-μl fractions were collected. Radioactivity was determined by Cerenkov counting of fractions.

derived from the β subunit by reversed phase HPLC. In addition to a large peak in the breakthrough of the column, there were five labeled peptides resolved. Detailed analysis of these peptides will be presented elsewhere, but it is relevant here that, although some peaks (particularly 4 and 5) became more radioactive after treatment with AMPKK, the same peaks were also observed in the absence of AMPKK.

DISCUSSION

Although we did not quite achieve purification to homogeneity, the purification procedure for AMPKK described here is a great improvement over that previously available (24). We had originally observed that AMPK reactivating activity was still present in the AMPK preparation at the second step (DEAE-Sepharose) but that AMPK and AMPKK were completely resolved during the third step (blue-Sepharose). However, the development of the more quantitative AMPKK assay described here allowed us to monitor the recovery of AMPKK during the early stages of the preparation and revealed that the majority of the AMPKK activity was not in the 2.5–6% PEG pellet used to purify AMPK but rather in the 6% PEG supernatant in the first step, which we had previously discarded. Purifying AMPKK from the 6–10% PEG pellet resulted in a much greater recovery of active AMPKK. The final preparation was still contaminated with protein kinase(s), which slowly phosphorylated the SAMS peptide, but AMPK was completely absent by several criteria. Utilization of AMARA for monitoring reactivation of AMPK during the AMPKK assay overcame the problem of the high blanks obtained due to the presence of the SAMS kinase(s).

Remarkably, the degree of reactivation of AMPK using highly purified preparations of AMPKK was linear with the amount of AMPKK added, right up to 100% reactivation (Fig. 1). This suggests that AMPKK has a very low apparent K_m for AMPK, so that the rate does not fall although the concentration of dephospho-AMPK is dropping. The fact that AMPK and AMPKK seem to form a stable complex as judged by co-immunoprecipitation (see below) may be another reflection of high affinity binding between AMPK and AMPKK. Using cruder preparations of AMPKK (postmitochondrial supernatant or 6–10% PEG precipitate), the assay became nonlinear when reactivation was >30% (Fig. 1). This may either be due to the presence of inhibitors of reactivation or due to the fact that at these early stages in the preparation (prior to the blue-Sepharose) AMPKK is still contaminated with AMPK and that this is not completely corrected by running blanks in which exogenous dephosphorylated AMPK is omitted.

Utilizing AMPKK purified as far as step 5 (Mono Q) in the present preparation, we have already shown that reactivation of AMPK is completely dependent on the presence of AMP (25). We now report that, using a fixed concentration of 100 μM AMP, ATP inhibited the AMPKK reaction at high concentrations. This demonstrates for the first time that high concentrations of ATP inhibit the activation of AMPK by phosphorylation as well as causing direct allosteric inhibition of AMPK by binding at the allosteric site as reported previously (11, 25). Although alternative models are possible, the results in Fig. 6 could be interpreted via a model in which ATP bound to the catalytic site(s) on AMPKK at low concentrations (half-maximal effect at 16 ± 6 μM; this is within the range of apparent K_m values for ATP for other protein kinases) and at an inhibitory site at high concentrations (half-maximal effect at 360 ± 80 μM). However, with the present data it is not possible to distinguish between enzyme (AMPKK)-mediated and substrate (AMPK)-mediated effects of ATP. Elsewhere we have demonstrated that AMPKK is directly activated by AMP (27), raising the possibility that it is related to AMPK and that both AMPK and AMPKK may have two sites (catalytic and allosteric) for ATP. The biphasic curve in Fig. 3 may therefore reflect binding of ATP to multiple sites on both AMPKK and AMPK. Whatever the exact mechanism, these results show that high ratios of AMP to ATP would promote phosphorylation of AMPK by AMPKK (as long as there was sufficient ATP to satisfy its requirements as a substrate for AMPKK), whereas low ratios of AMP to ATP would inhibit phosphorylation of AMPK. The present observations in a cell-free system therefore parallel previous observations in intact cells that heat shock, arsenite, and other stresses that elevate the AMP:ATP ratio stimulate the activation of AMPK by phosphorylation (8).

Although conclusive identification of the catalytic subunit of AMPKK will have to await cDNA cloning and sequencing, the data in Figs. 3 and 7 strongly suggest that the catalytic subunit is a 58-kDa polypeptide (p58). Although other polypeptides could be detected in the preparation, p58 was the only polypeptide that was significantly labeled using [γ-^{32}P]ATP and [^{14}C]FSBA, both of which were used previously to identify the catalytic subunit of AMPK (11). In addition, ^{32}P-labeled p58 co-precipitated with AMPK, using antibody against the β subunit of the latter (Fig. 7). Precipitation of p58 did not occur unless AMPK was present, showing that it was not due to a chance cross-reaction between p58 and the AMPK-β antibody. As well as co-precipitating p58, the anti-AMPK-β antibody precipitated AMPKK activity, based on two separate analyses (data not shown): (a) in four separate incubations, 42 ± 8% (mean ± S.E.) of AMPKK activity was depleted from the supernatant after immunoprecipitation; (b) when a mixture of dephosphorylated AMPK and AMPKK were immunoprecipitated in the *absence* of MgATP, the subsequent addition of MgATP to the precipitate resulted in 4-fold reactivation of the AMPK, relative to a control in which AMPKK was not included. Thus, both p58 and AMPKK activity could be co-precipitated with AMPK, suggesting that the two are related. Whatever their relationship, these data demonstrate that AMPK and AMPKK form a complex that is stable during extensive washing of the immunoprecipitate.

We have previously reported that both AMPKK and AMPK are directly activated by AMP (27). This study reveals further similarities between the upstream and downstream protein kinases. The molecular masses of the catalytic subunits (AMPKK *versus* AMPK, 58 *versus* 63 kDa), the Stokes radii (5.5–5.7 *versus* 5.4–5.8 nm), the sedimentation coefficients (8.4–8.6 *versus* 7.9–8.4 S), and the estimated native molecular masses (196 ± 5 kDa *versus* 190 ± 10 kDa) are all very similar. The frictional ratios (f/f_0, 1.44–1.47 *versus* 1.46–1.50) also indicate that both are highly asymmetric molecules. This raises

the possibility that, like AMPK, which consists of α (63-kDa), β (38-kDa) and γ (35-kDa) subunits, AMPKK might also contain additional subunits as well as the 58-kDa catalytic subunit. No obvious candidates for these were seen in a Coomassie-stained gel of the immunoprecipitate shown in Fig. 7, but they could have been obscured by the subunits of AMPK and/or by the heavy or light chains of the immunoglobulin. Whatever the structure of the AMPKK oligomer, migration on a gel filtration column was not affected by the presence or absence of 0.2 M NaCl in buffer B, indicating that the oligomer is stable under these conditions.

In this study we identify threonine 172 as the major site phosphorylated by AMPKK on AMPK-α, leading to activation of AMPKK. We believe that all three radioactive peptide peaks that were labeled only after incubation with AMPKK are derived from this site. Trifluoroacetic acid peaks 5–7 eluted very close together (Fig. 8) and also yielded three closely eluting peaks on HPLC in ammonium acetate pH 6.5 (AA1–AA3, not shown). Although we did not have sufficient AA3 for sequence studies, AA1 and AA2 gave identical sequences, corresponding to the tryptic peptide commencing at Ile^{155} in AMPK-α_1 or AMPK-α_2, and in both cases the major radioactive amino acid was at cycle 18, corresponding to Thr^{172}. We suspect that trifluoroacetic acid peaks 5–7 (corresponding to AA1–AA3) are generated by differing degrees of oxidation of the two methionines within the peptide.

At least four other ^{32}P-labeled tryptic peptide peaks (Fig. 8, *peaks 1–4*) were separated from AMPK-α, but these were not affected by the presence of AMPKK and appear to be autophosphorylation sites that are phosphorylated independently of the state of activation of AMPK.

New information to be taken into account was the report (14), published just as we were about to submit this work, that rat liver AMPK catalytic subunit was encoded by not one but at least two genes, termed α_1 and α_2. The α_2 isoform seems to be expressed at a high level in rat liver, but it appears to have a low SAMS peptide activity, with α_1 apparently accounting for at least 90% of the SAMS peptide kinase activity in this tissue (14). The AMPK used for our identification of the phosphorylation site may have been a mixture of both isoforms, although because it had been purified on the basis of activity it presumably contained a substantial proportion of α_1. However, the sequence around Thr^{172} is perfectly conserved between α_1 and α_2, suggesting that AMPKK is likely to activate both forms. The predicted tryptic peptides containing this site (even allowing for failure to cleave at Arg^{171}) are also identical for both isoforms. Since the anti-β subunit antibody used for immunoprecipitation depletes all of the AMPK activity from even relatively crude preparations of rat liver (data not shown) it seems likely that it would precipitate both α_1 and α_2. Although we therefore cannot be certain whether the amino acid sequence containing Thr^{172} was derived only from α_1 or from both α_1 and α_2, our overall conclusions are not affected.

In contrast to the autophosphorylation sites on AMPK-α, the β subunit is more highly phosphorylated in the presence of AMPKK (Fig. 7). More detailed studies on the phosphorylation of the β subunit will be presented elsewhere, but current evidence[2] favors the idea that this is due to autophosphorylation and is not catalyzed by AMPKK.

Although further studies (*e.g.* site-directed mutagenesis) will be required to conclusively demonstrate that activation of AMPK by AMPKK is accounted for entirely by phosphorylation of Thr^{172}, comparison with other protein kinases lends considerable support to this hypothesis. AMPK joins a long list of protein kinases known to require phosphorylation within the "activation segment" (43) between the "DFG" motif (subdomain VII (41)) and the "APE" motif (subdomain VIII) for activity. The phosphorylation site on protein-serine/threonine kinases is usually a threonine but can also be tyrosine (Gsk3), threonine and tyrosine (mitogen-activated protein kinases), or two serines (mitogen-activated protein kinase kinases). In some cases, such as cyclic AMP-dependent protein kinase, these phosphate groups may be inserted during protein synthesis and appear to be stable *in vivo*. In many other cases such as Cdc2, mitogen-activated protein kinases, mitogen-activated protein kinase kinases, p90 ribosomal protein S6 kinase and AMPK, the phosphorylation can be readily reversed and has important regulatory consequences *in vivo*. In the crystal structure of the Cα subunit of cyclic AMP-dependent protein kinase, the phosphorylated threonine (Thr^{197}) interacts with a positively charged cluster (His^{87}, Arg^{165}, and Lys^{189}), thus permitting proper orientation of the pseudosubstrate peptides for phosphate transfer from ATP (43). Two of these three basic residues are conserved in AMPK-α1 and -α2 (12, 14).

The yeast (*S. cerevisiae*) homologue of AMPK, Snf1p, is inactivated by treatment with protein phosphatases and can be reactivated by treatment with a crude preparation of mammalian AMPKK (22), indicating that it may be regulated by phosphorylation at the site equivalent to Thr^{172}. A threonine residue (Thr^{210}) is conserved at this position in Snf1p, and the sequence around it is also highly conserved, with a few conservative replacements on the N-terminal side. Estruch *et al.* (44) have already shown that a T210A mutant is nonfunctional in yeast *in vivo* with respect to growth on raffinose or expression of invertase. This is entirely consistent with Thr^{210} being the site on Snf1p phosphorylated by a putative "Snf1p kinase," which is currently uncharacterized.

Calmodulin-dependent protein kinase I (CaMKI) is activated by phosphorylation by an upstream protein kinase (CaMKI kinase), and CaMKI kinase can also phosphorylate and activate calmodulin-dependent protein kinase IV, at least *in vitro*. The sites of regulatory phosphorylation modified by CaMKI kinase have been shown to be Thr^{177} (CaMKI (45)) and Thr^{196} (calmodulin-dependent protein kinase IV (46)), which exactly align with Thr^{172} on AMPK. We have recently shown that, although AMPKK and CaMKI kinase are distinct enzymes, AMPKK can slowly phosphorylate and reactivate CaMKI, while CaMKI kinase can slowly phosphorylate and reactivate AMPK (27). These observations are entirely consistent with our identification of Thr^{172} as the regulatory site on AMPK, given the relatively high sequence similarity of AMPK and CaMKI within the activation segment. Whether AMPKK can phosphorylate and activate other protein kinases more distantly related to AMPK than CaMKI remains to be determined.

Acknowledgments—We thank Fiona Smith for assistance with production of anti-β subunit antibodies; Tricia Cohen for PP1 and PP2C; and David Barford, Steve Keyse, and Nick Morrice for LAR, CL-100, and $PP2A_1$, respectively.

REFERENCES

1. Hardie, D. G., Carling, D., and Halford, N. G. (1994) *Semin. Cell Biol.* **5,** 409–416
2. Clarke, P. R., and Hardie, D. G. (1990) *EMBO J.* **9,** 2439–2446
3. Gillespie, J. G., and Hardie, D. G. (1992) *FEBS Lett.* **306,** 59–62
4. Munday, M. R., Campbell, D. G., Carling, D., and Hardie, D. G. (1988) *Eur. J. Biochem.* **175,** 331–338
5. Davies, S. P., Carling, D., Munday, M. R., and Hardie, D. G. (1991) *Eur. J. Biochem.* **203,** 615–623
6. Sim, A. T. R., and Hardie, D. G. (1988) *FEBS Lett.* **233,** 294–298
7. Carling, D., and Hardie, D. G. (1989) *Biochim. Biophys. Acta.* **1012,** 81–86
8. Corton, J. M., Gillespie, J. G., and Hardie, D. G. (1994) *Curr. Biol.* **4,** 315–324
9. Davies, S. P., Hawley, S. A., Woods, A., Carling, D., Haystead, T. A. J., and Hardie, D. G. (1994) *Eur. J. Biochem.* **223,** 351–357
10. Stapleton, D., Gao, G., Michell, B. J., Widmer, J., Mitchelhill, K., Teh, T.,

[2] S. A. Hawley, M. Davison, A. Woods, S. P. Davies, R. K. Beri, D. Carling, and D. G. Hardie, unpublished observations.

House, C. M., Witters, L. A., and Kemp, B. E. (1994) *J. Biol. Chem.* **269,** 29343–29346
11. Carling, D., Clarke, P. R., Zammit, V. A., and Hardie, D. G. (1989) *Eur. J. Biochem.* **186,** 129–136
12. Carling, D., Aguan, K., Woods, A., Verhoeven, A. J. M., Beri, R. K., Brennan, C. H., Sidebottom, C., Davison, M. D., and Scott, J. (1994) *J. Biol. Chem.* **269,** 11442–11448
13. Mitchelhill, K. I., Stapleton, D., Gao, G., House, C., Michell, B., Katsis, F., Witters, L. A., and Kemp, B. E. (1994) *J. Biol. Chem.* **269,** 2361–2364
14. Stapleton, D., Mitchelhill, K. I., Gao, G., Widmer, J., Michell, B. J., Teh, T., House, C. M., Fernandez, C. S., Cox, T., Witters, L. A., and Kemp, B. E. (1996) *J. Biol. Chem.* **271,** 611–614
15. Gao, G., Widmer, J., Stapleton, D., Teh, T., Cox, T., Kemp, B. E., and Witters, L. A. (1995) *Biochim. Biophys. Acta.* **1266,** 73–82
16. Beri, R. K., Marley, A. E., See, C. G., Sopwith, W. F., Aguan, K., Carling, D., Scott, J., and Carey, F. (1994) *FEBS Lett.* **356,** 117–121
17. Celenza, J. L., Eng, F. J., and Carlson, M. (1989) *Mol. Cell. Biol.* **9,** 5045–5054
18. Fields, S., and Song, O. K. (1989) *Nature* **340,** 245–246
19. Yang, X., Jiang, R., and Carlson, M. (1994) *EMBO J.* **13,** 5878–5886
20. Yang, X., Hubbard, E. J., and Carlson, M. (1992) *Science* **257,** 680–682
21. Celenza, J. L., and Carlson, M. (1986) *Science* **233,** 1175–1180
22. Woods, A., Munday, M. R., Scott, J., Yang, X., Carlson, M., and Carling, D. (1994) *J. Biol. Chem.* **269,** 19509–19515
23. Moore, F., Weekes, J., and Hardie, D. G. (1991) *Eur. J. Biochem.* **199,** 691–697
24. Weekes, J., Hawley, S. A., Corton, J., Shugar, D., and Hardie, D. G. (1994) *Eur. J. Biochem.* **219,** 751–757
25. Corton, J. M., Gillespie, J. G., Hawley, S. A., and Hardie, D. G. (1995) *Eur. J. Biochem.* **229,** 558–565
26. Davies, S. P., Helps, N. R., Cohen, P. T. W., and Hardie, D. G. (1995) *FEBS Lett.* **377,** 421–425
27. Hawley, S. A., Selbert, M. A., Goldstein, E. G., Edelman, A. M., Carling, D., and Hardie, D. G. (1995) *J. Biol. Chem.* **270,** 27186–27191
28. Alessi, D. R., Street, A. J., Cohen, P., and Cohen, P. T. W. (1993) *Eur. J. Biochem.* **213,** 1055–1066
29. Streuli, M., Krieger, N. X., Hall, L. R., Schlossmann, S. F., and Saito, H. (1988) *J. Exp. Med.* **168,** 1553–1562
30. Keyse, S. M., and Emslie, E. A. (1992) *Nature* **359,** 644–647
31. Cohen, P., Alemany, S., Hemmings, B. A., Resink, T. J., Strålfors, P., and Lim, T. H. (1988) *Methods Enzymol.* **159,** 390–408
32. Dale, S., Wilson, W. A., Edelman, A. M., and Hardie, D. G. (1994) *FEBS Lett.* **361,** 191–195
33. Woods, A., Cheung, P. C. F., Smith, F. C., Davison, M. D., Scott, J., Beri, R. K., and Carling, D. (1996) *J. Biol. Chem.* **271,** 10282–10290
34. Davies, S. P., Carling, D., and Hardie, D. G. (1989) *Eur. J. Biochem.* **186,** 123–128
35. Bradford, M. M. (1976) *Anal. Biochem.* **72,** 248–254
36. Laemmli, U. K. (1970) *Nature* **227,** 680–685
37. Matsudaira, P. (1987) *J. Biol. Chem.* **262,** 10035–10038
38. Coull, J. M., and Pappin, D. J. C. (1990) *J. Prot. Chem.* **9,** 259–264
39. Haystead, C. M. M., Gregory, P., Sturgill, T. W., and Haystead, T. A. J. (1993) *Eur J. Biochem* **214,** 459–467
40. Zoller, M. J., Nelson, N. C., and Taylor, S. S. (1981) *J. Biol. Chem.* **256,** 10837–10842
41. Hanks, S. K., and Hunter, T. (1995) in *The Protein Kinase FactsBook* (Hardie, D. G., and Hanks, S. K., eds) Vol. 1, pp. 7–47, Academic Press, London
42. Siegel, L. M., and Monty, K. J. (1966) *Biochim. Biophys. Acta.* **112,** 346–362
43. Johnson, L. N., Noble, M. E. M., and Owen, D. J. (1996) *Cell* **85,** 149–158
44. Estruch, F., Treitel, M. A., Yang, X., and Carlson, M. (1992) *Genetics* **132,** 639–650
45. Haribabu, B., Hook, S. S., Selbert, M. A., Goldstein, E. G., Tomhave, E. D., Edelman, A. M., Snyderman, R., and Means, A. R. (1995) *EMBO J.* **14,** 3679–3686
46. Selbert, M. A., Anderson, K. A., Huang, Q.-H., Goldstein, E. G., Means, A. R., and Edelman, A. M. (1995) *J. Biol. Chem.* **270,** 17616–17621

Characterization of the AMP-activated Protein Kinase Kinase from Rat Liver and Identification of Threonine 172 as the Major Site at Which It Phosphorylates AMP-activated Protein Kinase

Simon A. Hawley, Matthew Davison, Angela Woods, Stephen P. Davies, Raj K. Beri, David Carling and D. Grahame Hardie

J. Biol. Chem. 1996, 271:27879-27887.
doi: 10.1074/jbc.271.44.27879